The preparation, structure and magnetic separation characteristics of high-ferric and low-alkali content red mud

Hui-bin Yang[1], Shu-zhen Zhang[2], Xiao-lin Pan[3]

1. Chief engineer of alumina research institute, Zhengzhou Non-ferrous Metals Research Institute Co., Ltd of CHALCO, Zhengzhou China
2. Senior engineer of chemical alumina, Shandong Research Institute of CHALCO, Zibo 255051, China
3. Director of department of nonferrous metals, School of Metallurgy, Northeastern University, Shenyang 110819, China

Corresponding author：yhuibin@126.com

Abstract

The red mud, obtained from high-ferric gibbsitic bauxite digested in alkaline solution with atmospheric pressure, has loose structure and small particle size. Besides, the contents of Fe_2O_3 and Na_2O in the low-alkali red mud are 64.74% and 1.25%, respectively. And Goethite and hydrated hematite account for a large proportion, the latter coming from the hydration reaction in bauxite digestion process. This research aims to study the mineral structure and magnetic concentration properties of one kind of high-ferric and low-alkali red mud, using several modern testing methods such as X-ray diffraction (XRD), scanning electron microscopy (SEM), infrared spectroscopy (IR) and Brunauer–Emmett–Teller (BET) surface-area measurements. Analysis demonstrates that the suitable magnetic field intensity is 6000 GS, under which condition, the yield of concentrate is 46.42% and the Fe accounts for 52.84%. Besides, the concentrate have lower Na_2O content and higher Fe_2O_3 content, which can be used for the raw material of ironworks.

Keywords: high-ferric and low-alkali, red mud, atmospheric pressure digestion, structure, magnetic separation.

1. Introduction

Red mud, one kind of alumina industrial residue, is produced after gibbsitic bauxite digested in the Bayer process. Hematite, goethite and desilication product (DSP) are the main components of red mud in the traditional Bayer processred mud. In addition, red mud also contains a small amount of other mineral components like boehmite, quartz, anatase, and so on. The traditional digestion temperature and pressure are 145 °C and 5 kg/cm^2, respectively. DSP, produced in the digestion process, is hard to separate. Traditional Bayer red mud contains 8-15% Na_2O, which pollutes water, soil, and atmosphere. And this is the reason why red mud cannot be used widely. According to the statistics, the annual output of red mud is more than 70,000,000 tons in the world. How to deal with red mud is always one global problem [1, 2].

The research of traditional Bayer red mud focuses on iron selection [3, 4], as a building material or filler [5], recycling valuable components or elements [6-8] and so on. Literatures show that Bayer red mud also can be used for mineral thickening material or filling in cement [9, 10], made into non-sintering brick and porous ceramic filter ball [11, 12]. Besides, in some area, the red mud may contain higher scandium (Sc), which can be used to extract Sc_2O_3 by solution extraction [13]. In addition, the Al_2O_3 and Na_2O can be recovered from red mud in the sintering process red mud, and Central South University has studied how to extract Al_2O_3 from red mud by sintering process [14].

Xinqin L. and Laishi L. declared that sintering process could be used to extract Al_2O_3 from red mud high-efficiency and Bayer-sintering series process was the best process to deal with low grade bauxite [15, 16]. Jiadong H. etc. studied the technic of extracting alumina from red mud in lab [17]. Besides, some researchers even studied the sintering process like sintering temperature, desilication confluence position, sintering thermal regulation, composition of the clinker and so on [18, 19].

Fe_2O_3, as the maximum component in the red mud which makes extract iron from red mud, has been the main research direction. Guangxi Pingguo alumina refinery began to work on research of the Bayer red mud separation iron technology in 2008, whose industry production line were built in June 2011 and the pulsating high gradient two-stage magnetic separation technology were used in the item. The iron (Fe) content of concentrate can reach 55%, which can be used for the raw material of iron refinery. Yingbang X. et al. also studied reduction smelting iron separation technology of the Pingguo red mud [20], in which Red mud and coke mixed together to smelt, with the ratio of coke vs red mud to be 2.65, and the recovery ratio of the Fe can reach 97%.

Yanfei Z. applied hydrophobic agglomeration and magnetic seed iron separation technology to deal with Bayer red mud [21]. The iron content of the red mud sample is about 24% and the effects of magnetic field intensity, stirring speed, dispersing agent, quantity of the magnetic seed, and flocculating agent on the magnetic separation were studied. Maybe the selective hydrophobic flocculation magnetic separation is the best method to deal with fine particle red mud, because the iron content of concentrate can reach 50.62% and the recovery ratio of Fe can be 45.97%. Qunhu X. et al. used coal powder to reduce Pingguo Bayer red mud, besides the magnetic separation was applied [22]. The iron content of concentration sample is 54.51% and the recovery ratio of the iron is 55.01%. Wenchen J. studied how to extract Fe_2O_3 and Al_2O_3 from red mud by soda-lime sintering process [23]. Wanchao L. etc. studied the technology of red mud reducing roasting with adding coal and magnetic separation. The metallization ratio of Fe_2O_3 can reach 96.98% and recovery ratio is 81.40%. The tailings of the magnetic separation can be used as building material [24, 25]. Qi D. used high gradient permanent magnet separation technology to deal with red mud [26]. The Fe_2O_3 content of concentrate can reach 69.28% and the recovery ratio of red mud and Fe_2O_3 are 24.96% and 58.12%, respectively. In addition, other researchers also studied how to separate Fe_2O_3 from red mud by some methods, like hydrothermal, calcination, reduction smelting, magnetic-separation and so on [27-29].

The red mud, produced in atmospheric pressure (normal pressure, digestion temperature is 95-105 °C), contains no or only less DSP. This red mud is suitable to comprehensive utilization for its higher Fe_2O_3 content and lower contents of Na_2O and Al_2O_3 [30]. The structure of red mud was studied through various detecting methods; besides preliminary magnetic separation tests were conducted. Those results can be used as the reference for red mud comprehensive utilization and the improvement of gibbsitic bauxite digestion technology.

2. Material and Methods

2.1 Material

High-ferric gibbsitic bauxite was selected to produce high-ferric red mud, which was obtained from Kalimantan, Indonesia. The sample was dried at 105 °C for 6 hours, and then crushed by a jaw crusher and roll-crushing mill. The particle size of final sample was between 0.5 and 1.0 mm. Detailed information of the sample are shown in Table 1, Table 2, and Figure 1.

Table 1. Main chemical compositions of high-ferric gibbsitic bauxite (mass, %).

SiO_2	Fe_2O_3	Al_2O_3	TiO_2	**Loss on Ignition**
2.78	31.03	39.30	1.01	22.60

Table 2. Mineral compositions of high-ferric gibbsitic bauxite (mass, %).

Gibbsite	Hematite	Goethite	Kaolinite	Quartz	Anatase
47.50	20.20	22.65	5.25	0.30	1.01

As shown in Table 1, the content of Fe_2O_3 is 31.03% and SiO_2 is 2.78%, which is superior quality high-ferric and low-silica gibbsitic bauxite.

As shown in Table 2, gibbsite, hematite and goethite are the main minerals. The content of kaolinite is 5.25%. Kaolinite influences bauxite digestion process seriously, because the SiO_2 in the kaolinite will participate in reaction. The more the SiO_2 content is, the easier desilication reaction is and the higher Na_2O content in the red mud is. Whereas, the lower the SiO_2 content in the bauxite is, the lower the Na_2O content in red mud is.

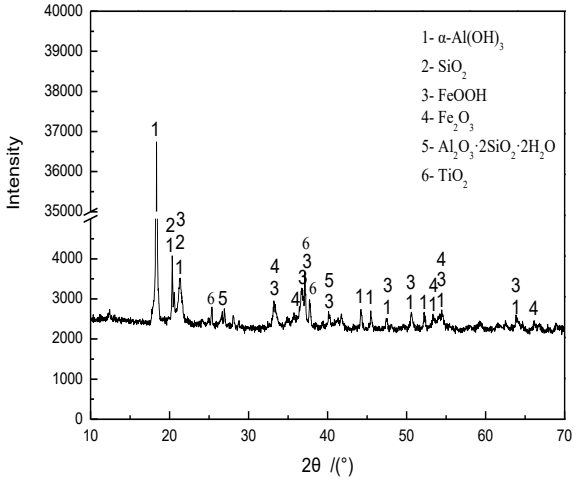

Figure 1. XRD pattern of high-ferric gibbsitic bauxite.

Testing results of XRD is in accord with the results of bauxite quantitative analysis. Gibbsite is the main mineral, and at the same time hematite, goethite, quartz also exist in the bauxite.

2.2. Test Instruments and Methods

The atmospheric pressure digestion test was carried out in three-hole flask. The concentration of NaOH in alkali solution was 3 mol/L and the mass ratio of solid vs solution was 1:10. The flask was put into one thermostatic water bath, where temperature was 92 °C (actual digestion temperature was 90 °C, the temperature difference of flask inside and outside was 2 °C) and the digestion duration time was 60 minutes. In order to ensure digestion temperature, the liquid level in the water bath was higher than the solution level in the flask. Mechanical stirrer was used in the experiment and stirring speed was 350 r/min. The stirring rod was placed in the middle hole of the flask. In order to control evaporation of the solution, one hole of the flask was equipped with

condenser tube and another hole had a thermometer for monitor reaction temperature. After digestion test, the digestion slurry was filtered and the red mud was washed, dried and then was used for analysis.

High pressure digestion test (low temperature Bayer process) was carried out in a homogeneous reactor. The concentration of NaOH was 3 mol/L and the mass ratio of solid vs solution was 1:10, which was same to atmosphere pressure digestion. The digestion temperature was 150 °C and duration time was 60 minutes. After filtration, washing and drying, the high pressure digestion red mud was used for analysis.

Wet magnetic separation was selected as the red mud magnetic separation test method. The mass ratio of red mud vs distilled water in the slurry was 5.0 and the magnetic field intensity of permanent magnetic separator was 6000 and 9000 GS, high magnetic product for high-ferric content concentrate and low magnetic product for tailings. The concentrates were dried directly and the tailings were dried after filtration, and then calculate concentrate production ratio. Both of the red muds were tested for chemical analysis and various physicochemical properties.

A D8 ADVANCE X-ray diffractometer with a Cu target cathode (Kα，λ=0.15418 nm) was used for the X-ray diffraction (XRD) analysis of the samples. The voltage was 30 kV, the current was 15 mA, the scanning angle was varied from 10° to 70°, and the scanning speed was 4 °/min.

Scanning electron microscopy (SEM) observations of the samples were performed on a S4800 cold field-emission scanning electron microscope equipped with an energy-dispersive X-ray spectroscopy (EDS) apparatus. The resolution ratio was 1.00 nm (15 kV), and the acceleration voltage was 0.50 to 30 kV.

The infrared spectra (IR) were obtained from a Spectrum400 Fourier transform infrared spectrometer. The frequency range was 400 to 25,000 cm^{-1}, and the resolution was 1 cm^{-1}.
The Brunauer–Emmett–Teller (BET) specific surface area was measured using a V-Sorb 2800P specific surface area and aperture analyzer. The specific surface area measurement range was greater than 0.01 m^2/g, and the aperture measurement range was 0.35–400 nm.

3. Results and Discussion

3.1 Preparation of High-Ferric Red Mud

High-ferric red mud was obtained after high-ferric gibbsitic bauxite digested under atmospheric pressure. The chemical compositions of high-ferric red mud were detected and shown in Table 3. The content of Fe_2O_3 reached 64.74% which is typical high-ferric red mud.

Table 3. Chemical compositions of red mud while digested under atmospheric pressure (mass, %).

SiO_2	Fe_2O_3	Al_2O_3	CaO	Na_2O	TiO_2
4.57	64.74	15.25	2.50	1.25	1.77

In order to contrastive analysis, the performance characteristics of the atmospheric pressure digestion red mud and high pressure digestion test were carried out. Chemical compositions of high pressure digestion red mud are shown in Table 4.

Table 4. Chemical compositions of red mud while digested under high pressure (mass, %).

SiO_2	Fe_2O_3	Al_2O_3	CaO	Na_2O	TiO_2
7.42	64.56	13.50	2.50	3.75	1.75

Shown as Table 3 and 4, the contents of Na_2O and SiO_2 were higher in Table 4 than that of Table 3. It is because of the desilication reaction occurring more serious in the high pressure digestion process. The desilication reaction equation was shown as equation (1) [31]:

$$2\mathrm{NaAl}(OH)_4 + xNa_2H_2SiO_4 + aq = Na_2O.Al_2O_3.xSiO_2.nH_2O + 2xNaOH + aq \quad (1)$$

Desilication reaction made the red mud contains DSP, which will lead to more Na_2O and SiO_2 appears in the red mud. Contents of SiO_2 are 7.42% and 4.57% in high pressure and atmospheric pressure digestion red mud, respectively. Content of Na_2O is 3.75% in high pressure digestion red mud, which is three times the amount of Na_2O in atmospheric pressure digestion red mud.

The content of Na_2O in atmospheric pressure red mud decreased 66.67% contrast with high pressure red mud, which was beneficial for the application of atmospheric pressure red mud.

3.2 Mineral Structure and Properties of High-Ferric Red Mud

XRD pattern of high-ferric red mud is shown in Fig. 2. It can be seen that the main minerals are goethite, hydrated hematite, gibbsite, small amount of titanium oxide and hydrated sodium aluminosilicate in the red mud. Characteristic peaks of gibbsite as shown in Fig. 2, which indicate the bauxite did not digest completely under atmospheric pressure. Bauxite digestion ratio can get improved by increasing reaction temperature or NaOH concentration. The goethite in the red mud comes from raw bauxite. A large Amount of hematite contained in the raw bauxite but no was found in the red mud. Instead, the characteristic peaks of hydrated hematite appeared in the red mud. This indicates that hematite may react with water and produce hydrated hematite in the process of digestion. Less amount of TiO_2 is come from raw bauxite. Less amount of DSP exist in the red mud indicates that tiny desilication participated in reaction during digestion process. Literatures indicate that crystal of hematite does not change when bauxite digest under low temperature (150 °C) Bayer process. In the red mud, Fe_2O_3 exist in the form of hematite, goethite or alumogoethite [32, 33]. The digestion temperature of atmospheric pressure was lower than that of low temperature Byer process, which made the red mud mineral composition, also conformed to this characteristic.

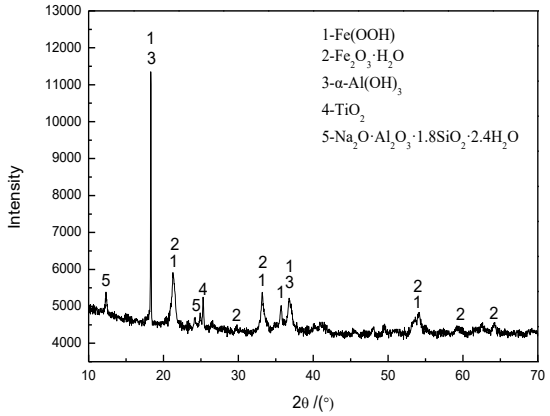

Figure 2. XRD pattern of red mud while digested under atmospheric pressure.

The XRD pattern of high pressure digestion red mud was shown in Fig. 3. Main minerals in the red mud were goethite, hydrated hematite, hydrated sodium aluminosilicate, and less titanium oxide. Contrasted with atmospheric pressure red mud, the characteristic peaks of gibbsite disappeared completely and the peaks of DSP becomes more obvious in Fig. 3, which indicates higher DSP content or better DSP crystal in the red mud.

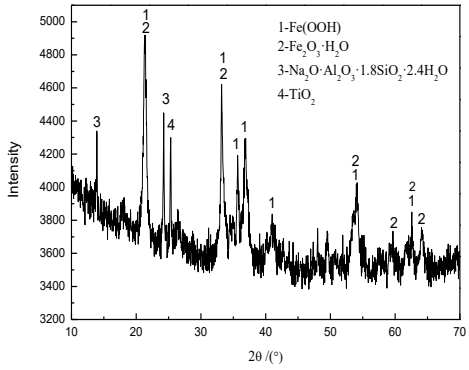

Figure 3. XRD pattern of red mud while digested under high pressure.

The SEM images of atmospheric digestion red mud were shown in Fig. 4. As shown in Fig. 4(a), a large amount of small particles (diameter less than 1 μm) was observed in the red mud, which is the reason why digestion slurry is hard to filtration. Literature reported that those particles were goethite, hematite, and other iron-bearing minerals [34]. As shown in Fig. 4(a), some particles had a flat surface, which should due to the particle agglomeration. As shown in Fig. 4(b), some flaky residue appeared in the red mud which should be undigested gibbsite crystal. These gibbsite crystals might be wrapped by other minerals which would lower its digestion speed more or less.

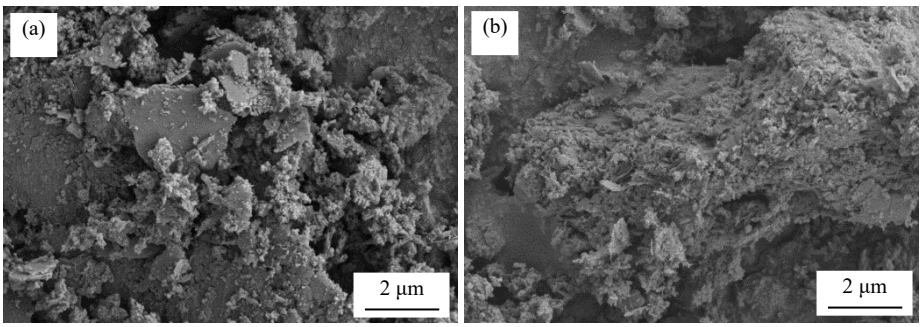

Figure 4. SEM images of red mud while digested under atmospheric pressure (a) scattered particles; (b) undigested flakes

After digestion under atmospheric pressure, the red mud was divided into large particles and tiny particles due to the difference of sedimentation rate. The red mud with large particles would drop towards bottom very fast and tiny particles would suspend in solution for a long time, which characteristic could be used to divide the two parts of them. SEM images of large particle and tiny particle were shown in Fig. 5 and 6, respectively. Shown as Fig. 5, the mineral shape in large particle looked like needle or stick. Some particles were looseness, shown as Fig. 5(a). And some were dense, shown as Fig. 5(b). According to the research results of gibbsitic bauxite structure, red mud structure and chemical compositions (Fig. 1, Fig. 2 and table 1, table 2), those minerals should be goethite and hematite. Most of tiny red mud particles size is less than 1 μm, shown as

Fig. 6(a). Some flaky gibbsite crystal particles appear in the tiny red mud particles, shown as Fig. 6(b).

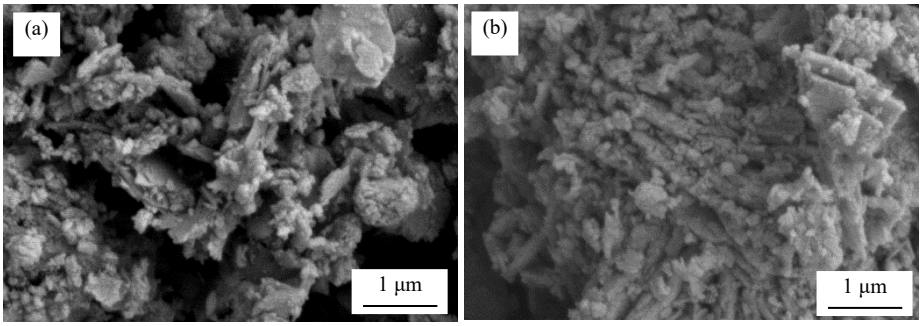

Figure 5. SEM images of large red mud particles while digested under atmospheric pressure (a) scattered needle-like particles; (b) needle-like aggregate particles.

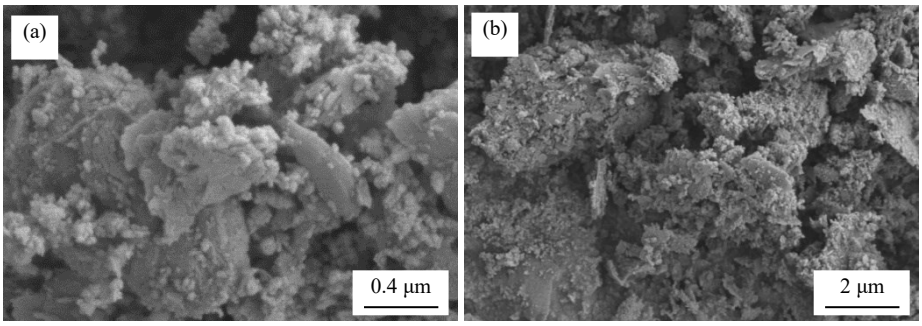

Figure 6. SEM images of tiny red mud particles while digested under atmospheric pressure (a) tiny particles; (b) flaky particles.

SEM images of high pressure (150 °C) digestion red mud was shown in Fig. 7. A large amount of tiny particles and particle aggregation were observed in Fig. 7. These minerals mainly are goethite and hematite, besides no undigested flaky gibbsite crystal was found in the image.

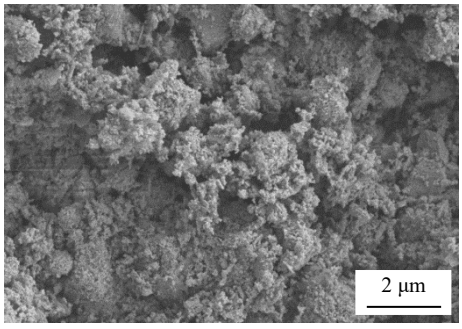

Figure 7. SEM images of red mud while digested under high pressure.

IR pattern of atmospheric pressure digestion red mud was shown in Fig. 8. The absorption peaks located among 3700-3000 cm^{-1} are symmetrical, and asymmetrical stretching vibration peaks of water molecules are mainly due to the hydrated hematite or crystal water of other minerals. The absorption peaks located between 797 cm^{-1} and 912 cm^{-1} are vibration peaks of Fe-OH, which

indicate the existence of goethite. Remaining absorption peaks were caused by other minerals in the red mud [35].

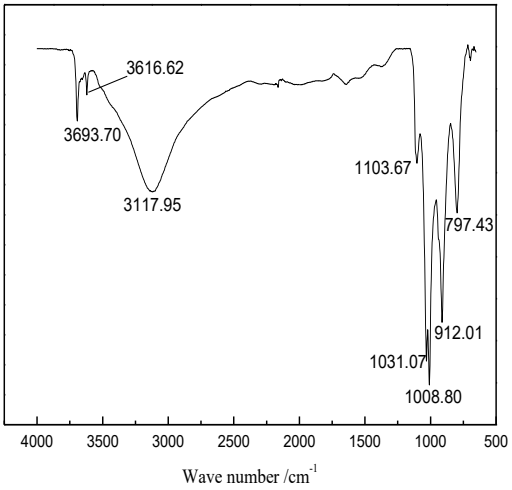

Figure 8. IR pattern of red mud while digested under atmospheric pressure.

The IR patterns of atmospheric pressure digestion red mud vs high pressure digestion red mud were shown in Fig. 9. Shown as Fig. 9, more absorption peaks appeared in the pattern of atmospheric pressure digestion red mud, which indicates the Mineral compositions are relatively complex. This should be the digestion reaction of the bauxite did not finish completely under atmospheric pressure.

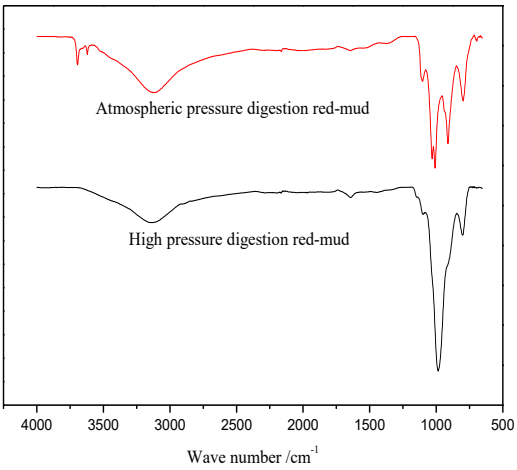

Figure 9. IR contrast patterns of atmospheric pressure and high pressure digestion red mud.

3.3 Magnetic separation properties and utilization of high-ferric red mud

The content of Fe_2O_3 in the high-ferric red mud was above 60%, which makes the red mud a higher value to extract Fe_2O_3. The Fe_2O_3 can be utilized effectively through magnetic separation, which can not only utilize the resources comprehensively, but also reduce the production cost of alumina.

Different kinds of red mud has differ beneficiation method. Magnetic separation may be the best choice when the content of quartz is high in red mud. Both magnetic separation and gravity separation are effectively when quartz is low in red mud. This is the reason why this paper focus on the study of magnetic separation technology used to deal with the red mud.
Magnetic field intensity should be between 5000～10000 GS when the minerals contains hematite and goethite. In this study, 6000 and 9000GS were selected to carry out the magnetic separation test.

Magnetic separation test results are shown in Table 5. When the magnetic field intensity is 9000 GS, the concentrate yield was 47.71% and the Fe_2O_3 content of concentrate was 74.66%. When the magnetic field intensity is 6000 GS, the concentrate yield was 46.42% and the Fe_2O_3 content of concentrate was 75.49%. Both of the above concentrates have higher Fe_2O_3 content than raw material, at the same time, the content of SiO_2 and Al_2O_3 decrease. In tailings, the content of SiO_2 and Al_2O_3 increases but the content of Fe_2O_3 decrease significantly. Test results demonstrate that the concentrate grade decreases when the concentrate yield increases, while the concentrate grade increases when the concentrate yield decreases. With comprehensive consideration, 6000 GS was selected as the appropriate magnetic intensity. The Fe content of concentrate was 52.84% while the magnetic field was 6000 GS. This kind of concentrate can partially substitute iron ore for the raw of iron-smelting.

Table 5. Magnetic separation results of high-ferric red mud (mass, %).

Sample	**Magnetic field intensity**	SiO_2	Fe_2O_3	Al_2O_3	CaO	**Concentrate yield**
High-ferric red mud		4.57	64.74	16.25	2.50	--
Concentrate	9000 GS	3.72	74.66	10.38	3.75	47.71
Tailing	9000 GS	7.03	56.03	21.25	3.75	--
Concentrate	6000 GS	3.64	75.49	9.75	3.75	46.42
Tailing	6000 GS	6.80	55.20	20.75	3.50	--

SEM images of concentrates and tailings were shown in Fig. 10. There was no obvious difference found between two kinds of concentrates and between two kinds of tailings. Compared with concentrate and tailings, concentrate particles were larger and the structure was denser relatively, tailings particles are relatively small and have a loose structure.

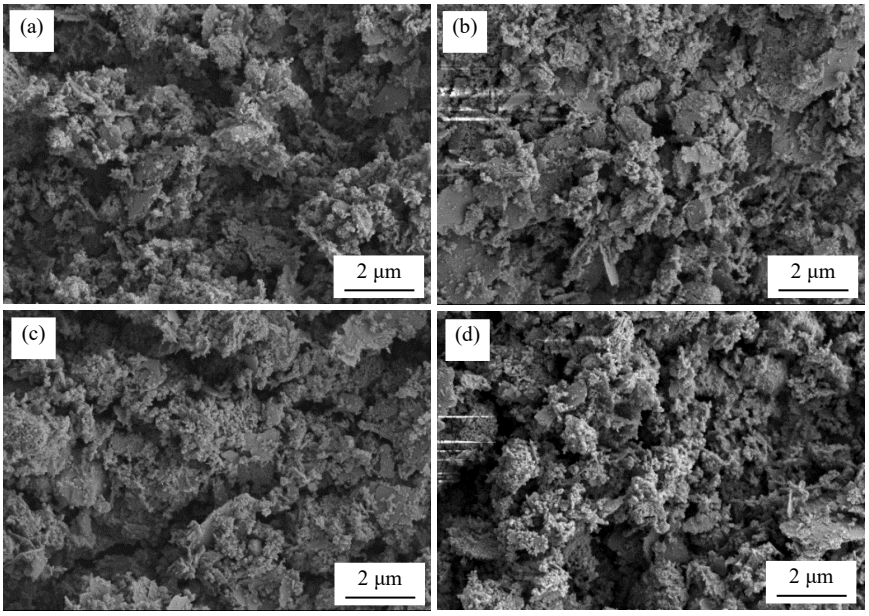

Figure 10. SEM images of concentrates and tailings (a) 9000 GS concentrate; (b) 9000 GS tailing; (c) 6000 GS concentrate; (d) 6000 GS tailing.

Pore volume and specific surface of 6000 GS magnetic separation concentrate and tailing were detected, shown in Table 6. The test data showed that the specific surface, pore volume and average pore diameter of tailing were larger than that of concentrate. There were two reasons leading to this results, one was the concentrate particle size was larger than tailing, another was the structure of concentrate was denser.

Several other technologies were also used in the process of red mud magnetic separation. Red mud reduction roasting was one of the considered technologies and has been reported in domestic literature [24, 36, 37]. It was roasting the mixture of red mud and coal to get clinker, and then using magnetic separation to deal with the fine-grained clinker. In this method, the Fe_2O_3 changed to Fe or Fe_3O_4, which can decrease the needed magnetic field intensity and improve the magnetic separation performance. But this method has a higher energy cost than magnetic separation directly. Therefore, red mud direct wet magnetic separation is a relatively economical and feasible technical method for industrial application.

Table 6. Specific surface area and pore volume of 6000 GS concentrate and tailing

Sample	Multipoint BET specific surface /$cm^2 \cdot g^{-1}$	Highest single-point adsorption total pore volume /$cm^3 \cdot g^{-1}$	Single-point total hole adsorption average pore diameter /nm
Concentrate	28.30	0.09	13.26
Tailing	33.52	0.15	17.44

4. Conclusions

The content of Fe_2O_3 and Na_2O in atmospheric pressure digestion red mud were 64.74% and 1.25%, respectively. It is typical high-ferric red mud. The content of Na_2O in atmospheric pressure digestion red mud was one third of the high pressure digestion red mud. Red mud containing lower Na_2O is convenient for comprehensive utilization.

Detection results show that main minerals were goethite and hematite in atmospheric pressure digestion red mud. A large amount of needle-shaped goethite crystal particles was observed. The hydrate hematite was found in the red mud, which due to the hematite hydration reaction during the atmospheric pressure digestion process.

The suitable magnetic field intensity for high-ferric red mud magnetic separation is 6000 GS. Under this condition, the concentrate yield was 46.42% and the Fe_2O_3 content of concentrate was 75.49% (converting into Fe accounts for 52.4%). The Fe_2O_3 content of concentrate increased compared with raw material, while the contents of SiO_2 and Al_2O_3 decreased. Particle size and structure of concentrate were larger and denser, while that of the tailings were just the opposite.

5. References

1. Wanjun Yao et al., Present research status of comprehensive utilization of red mud from Bayer process. *Inorganic Chemicals Industry*, Vol. 42, No. 12, (2010), 9-11.
2. M.E. Eliopoulos et al., Potential leaching of Cr(VI) from laterite mines and residues of metallurgical products (red mud and slag): An integrated approach. *Journal of Geochemical Exploration*, Vol. 162, No. 3, (2016), 40-49.
3. Yang Yang et al., Recovery of iron from red mud by selective leach with oxalic acid. *Hydrometallurgy*, Vol. 157, No. 10, (2015), 239-245.
4. Duncheng Fan et al., Orthogonal Experiments on Direct Reduction of Carbon-bearing Pellets of Bayer Red Mud. *Journal of Iron and Steel Research*, Vol. 22, No. 8, (2015), 686-693.
5. Rixin Liu et al., Utilization of red mud derived from bauxite in self-compacting concrete. *Journal of Cleaner Production*, Vol. 112, No. 1-1, (2016), 384-391.
6. Yanfang Huang et al., A perspective of stepwise utilisation of Bayer red mud: Step two-Extracting and recovering Ti from Ti-enriched tailing with acid leaching and precipitate flotation. *Journal of Hazardous Materials*, Vol. 307, No. 4, (2016), 318-327.
7. M. Urík et al., Aluminium leaching from red mud by filamentous fungi. *Journal of Inorganic Biochemistry*, Vol. 152, No. 11, (2015), 154-159.
8. R.A. Abdulvaliyev et al., 2015. Gallium and vanadium extraction from red mud of Turkish alumina refinery plant: Hydrogarnet process. *Hydrometallurgy*, Vol. 157, No. 10, (2015), 72-77.
9. Xiaoqin Peng et al., Preliminary Study of Bayer Red-mud as the Mineral Thickening Material for Mortar. *Journal of Hunan University (Natural Sciences)*, Vol. 36, No. 11, (2009), 16-20.
10. P.E. Tsakiridis et al., Red mud addition in the raw meal for the production of Portland cement clinker. *Journal of Hazardous Materials*, Vol. 116, No. 1/2, (2004), 103-110.
11. Jianjun Peng et al., Study on preparation and performance of unburned paving brick by Bayer red mud. *New Building Materials*, Vol. 38, No. 4, (2011), 21-23.
12. Su Zhao et al., Experimental Research of Bayer Red Mud Preparation of Porous Ceramic Filter Balls. *Journal of Shenyang Jianzhu University (Natural Science)*, Vol. 26, No. 2, (2010), 306-310.
13. Keqin Wang et al., Study on Removal of Aluminum and Extraction of Scandia from Shanxi Bayer Process Red Mud. *Chinese Rare Earths*, Vol. 33, No. 3, (2012), 78-81.
14. Qiusheng Zhou et al., 2008. Alumina recovery from red mud with high iron by sintering process. *Journal of Central South University (Science and Technology)*, Vol. 39, No. 1, (2008), 92-97.
15. Xinqin Liao et al., Series method is the best method for producing alumina in low-grade bauxite. *Collected papers of the symposium on environmental protection engineering and environmental risk prevention management of national nonferrous mines*, (2014), 104-106.
16. Laishi Li et al., The comparison of series and ore dressing Bayer method to product alumina with middle-low grade bauxite. *Light Metals*, No. 8, (2013), 16-19.

17. Jiadong Han et al., Test and study of alumina production with Series process. *Light Metals*, No. 10, (2007), 9-13.
18. Jianxin Liu, Discussion on sintering temperature in series process of producing alumina clinker. *World Nonferrous Metals*, No. 6, (2008), 28-31.
19. An'ling Han, Confluence desilication of alumina production in series process. *Light Metals*, No. 5, (2006), 24-26.
20. Yingbang Xie et al., Pilot-plant Test of Resource Utilization of Red Mud in Guangxi Pingguo Aluminum. *Nonferrous Metals (Extractive Metallurgy)*, No. 9, (2014), 30-33.
21. Yanfei Zhou, Study on the recovery of iron and mechanism from red mud by hydrophobic agglomeration and magnetic seed method. *Changsha: Central south University*. (2009).
22. Qunhu Xue et al., Experimental study of iron recovering from high iron contained red mud by Bayer process. *Journal of Mineralogy and Petrology*, Vol. 31, No. 4, (2011), 7-12.
23. Wenchen Jiang, Study on the recovery of iron and aluminum technology by soda-lime sintering method from Bayer red mud. *Wuhan: Huazhong University of Science and Technology*. (2009).
24. Wanchao Liu et al., Recovering iron and preparing building material with residues from Bayer red mud. *The Chinese Journal of Nonferrous Metals*, Vol. 18, No. 1, (2008), 187-192.
25. Guangfu Duan, The preparation of building materials and mechanism by Bayer alumina process waste residue. *Wuhan: Huazhong University of Science and Technology*. (2007).
26. Qi Deng et al., Experiment Research of Extracting Iron from Bayer Red Mud by Magnetic Separation Equipment. *Journal of Ceramics*, Vol. 33, No. 3, (2012), 365-371.
27. Zigao Liu et al., Treatment and utilization of Bayer process red mud. *The Chinese Journal of Nonferrous Metals*, Vol. 7, No. 1, (1997), 40-44.
28. L. Piga et al., Application of thermal analysis techniques to a sample of Red Mud by product of the Bayer process for magnetic separation. *Thermochimica Acta*, No. 254, (1995), 337-345.
29. Yongkang Liu et al., Study on coal-based direct reduction of high iron content red mud. *Sintering and Pelletizing*, Vol. 20, No. 2, (1995), 5-9.
30. Huibin Yang et al., Study of comprehensive utilization of gibbsite with high iron and low silicon. *Light metals*, No. 11, (2015), 12-18.
31. Shiwen Bi et al., Alumina production technology. *Beijing: Chemical Industry Press*, (2006), 65.
32. Wenmi Chen et al., A study on phase transition of goethite to hematite during digesting gibbsite-type bauxite. *Light Metals*, No. 2, (2012), 18-21.
33. Xiaobin Li et al., Effect of alumogoethite in Bayer digestion process of high-iron gibbsitic bauxite. *The Chinese Journal of Nonferrous Metals*, Vol. 23, No. 2, (2013), 543-548.
34. Huibin Yang, The Dissolution Process and Kinetics of High Iron Gibbsitic Bauxite under Normal Pressure. *Shenyang: Northeastern University*. (2016).
35. Shuai Wang et al., FTIR Spectroscopic Analysis of Cu2+ Adsorption on Hematite and Bayerite. *Spectroscopy and Spectral Analysis*, Vol. 31, No. 9, (2011), 2403-2406.
36. Yongfeng Sun et al., Technology for Recovering Iron from Red Mud by Bayer Process. *Metal Mine*, Vol. 39, No. 9, (2009), 176-178.
37. Shuren Liu, Reduction roasting - magnetic separation method to recover the iron from red mud. *Kunming: Kunming University of science and technology*. (2014).